

# Multi-Frequency Large-Signal Analysis Using Describing Functions

Scott Schafer, Zoya Popović  
 Electrical Computer and Energy Engineering  
 University of Colorado at Boulder  
 Boulder, Colorado 80309  
 Email: zoya@colorado.edu

**Abstract**—Describing functions are developed as a large-signal analysis tool for multi-frequency and multi-dimensional nonlinearities. The implementation and analysis method is discussed along with limitations. Describing functions are then used to analyze a GaN transistor in large-signal operation at X-band with a low frequency excitation on the drain for supply modulation. Describing functions agree well with harmonic balance over RF input power into saturation of the FET device and are used to characterize the FET baseband impedance with a second RF tone.

**Index Terms**—Describing functions, nonlinear analysis, large-signal analysis.

## I. INTRODUCTION

Previous efforts in modeling nonlinear elements have focused on Volterra series, e.g. [1]–[4], which can accurately describe only mildly nonlinear circuits, requiring low orders of mixing products. Extraction of the Volterra series requires that the nonlinearity be a power series or a Taylor series (for non-polynomial function) about a bias point. The fitting of the power series to the nonlinearity restricts that applicability for Volterra series to small-signal and weakly nonlinear circuits. In addition, the Volterra operators are *independent* of amplitude meaning that the solution obtained is linearized about a single static operating point.

Many practical nonlinearities arise in large-signal mode where the Volterra series approach is not valid. A particularly challenging large-signal case is the analysis of saturated high-efficiency PAs with supply modulation (envelope tracking). The active device is in this case driven by large signals in the RF gate input at the carrier frequency, simultaneously with large envelope-bandwidth signals in the drain supply input, as shown in Fig. 1. In this paper, modeling of the complicated  $I_{ds}(V_{gs}, V_{ds})$  nonlinearity of the FET transistor is performed using the describing function (DF) quasi-linearization method [5] in which the extracted functions are *dependent* on the size of input signals. This property is incredibly useful in that it can explain small-signal and large-signal phenomena in a single compact formula. However, describing functions rely on knowing the input waveform and the ability to integrate the nonlinear element equation. For microwave circuits, DFs have been successfully applied to finding the “sweet-spot” for IMDs in a transistor power amplifier [6].

## II. DESCRIBING FUNCTION FORMULATION

Quasi-linearization used with DFs refers to a method where the approximated output is a linear operation that depends on the input of a signal of finite size, requiring knowledge

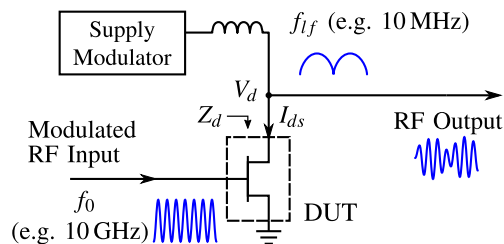


Fig. 1. Application for DF with multiple frequency excitations and mixing on the gate and drain of a nonlinear element for supply modulation.

of the type of input signal, as independent signals will *not* have independent outputs. Bias, sinusoidal, Gaussian noise are examples of types of inputs. The DF for a particular input form is the same for all nonlinearities. In microwave circuits, the input signal is generally a sum of sinusoidal signals at the input and output. This brings up an additional requirement that any feedback from the nonlinear output back to the input must be adequately filtered so the original input form still holds.

The DF for a single sinusoidal input to a real valued nonlinearity in phasor form can be written as [5]

$$N_1(V, \theta) = \frac{2}{2\pi} \int_0^{2\pi} y[V \cos(\phi)] e^{j\phi} d\phi, \quad (1)$$

where  $y[t]$  is the equation for the nonlinear element,  $\cos \phi$  is the input signal (in this case a sinusoid), and integration is carried out over all possible phases of the sinusoid  $\phi$ . The DF is dependent on the input amplitude and relative phase of the signal. The factor of 2 in the numerator accounts for two equal components at positive and negative frequencies. Equation (1) is mathematically simple and can easily be compared to Fourier series; the fundamental tone is being “picked” out of the signal  $y[x(t)]$  and the result becomes a *function* of the input amplitude and phase. Additionally, the  $n$ -th harmonic component at the output can be found easily:

$$N_n(V, \theta) = \frac{2}{2\pi} \int_0^{2\pi} y[V \cos(\phi)] e^{jn\phi} d\phi. \quad (2)$$

Equation (2) can be extended to a 2-dimensional nonlinear-

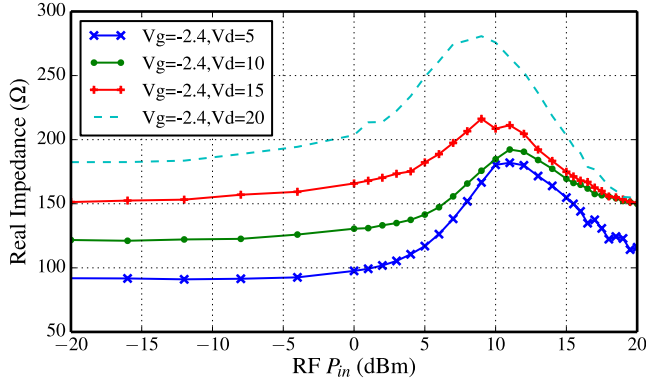


Fig. 2. Measured drain impedance at 1 MHz for a GaN FET device versus RF input power (10.7 GHz) and drain bias voltage. There is a characteristic peak in the low frequency impedance which occurs *before* the device saturates. The Angelov nonlinear model shows a similar effect versus RF input power.

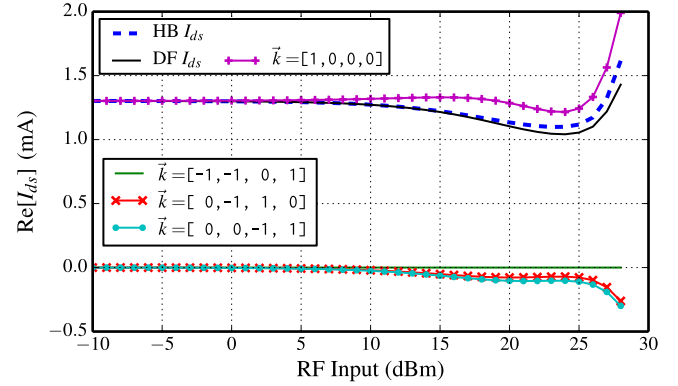


Fig. 3. Describing function result for Angelov FET with 10 GHz input on gate, and 10 MHz input on drain. The total DF result (sum of the individual mixing products) tracks very closely to the HB result (dotted blue line).

ity and  $K$ -sinusoidal inputs as follows

$$N_{\vec{k}}(\vec{V}_a, \vec{V}_b, \vec{\theta}_a, \vec{\theta}_b) = \frac{2}{(2\pi)^K} \int_0^{2\pi} d\phi_1 \cdots \int_0^{2\pi} d\phi_K y \left[ V_{a0} + \sum_{i=1}^K V_{ai} \cos(\phi_{ai} + \theta_{ai}), V_{b0} + \sum_{i=1}^K V_{bi} \cos(\phi_{bi} + \theta_{bi}) \right] \times \exp \left[ j \left( \sum_{i=1}^K k_i \phi_i \right) \right] \quad (3)$$

where  $K$  is the total number of input sinusoids,  $\vec{V}$  and  $\vec{\theta}$  are vectors of the input sinusoid amplitudes and phases respectively, and  $\vec{k}$  is a vector denoting the mixing order of the describing function. The subscripts  $a$  and  $b$  denote the two independent inputs to the nonlinearity (2-dimensional nonlinearity). Equation (3) also adds in the DC bias of  $V_0$  to the input of the nonlinear element. Even though (3) becomes a  $K$  dimensional integral, the interpretation is still simple; the full frequency spectrum (sum of tones) is fed to the nonlinear function ( $y[x(t)]$ ) and the  $\vec{k}$ -th order output is selected with the exponential ( $\exp(\dots)$ ).

If input frequencies are harmonics of one another, (3) is no longer the optimum DF. This is easily seen as the harmonics at the input of a nonlinear element can mix in different ways to the same output frequency. This means that *one* DF equation is no longer enough; the sum of all the mixing terms that land on a particular frequency is needed to get the total nonlinear response to the input tones.

The benefit of analyzing a nonlinear method with (3) as opposed to harmonic balance, is that the all mixing products at the same frequency can be computed, giving information about how the nonlinearity combines input tones to give the total harmonic response at a frequency. In contrast, harmonic balance gives only the total harmonic response.

### III. ANGELOV CURRENT SOURCE MIXING TONES

The interaction of a low frequency (LF) and RF signal in a nonlinear Angelov FET model is now examined on the example of a GaN FET which is operated in envelope tracking mode with a low-frequency 10-MHz large signal injected into the drain, while under large RF operation at 10 GHz. Using a Volterra series in this case is impractical because the signal amplitudes are large and the nonlinear current source equation is complicated, requiring a large number of coefficients. In the DF approach, the Angelov standard current source [7] replaces  $y[\dots]$  in (3), which is a function of the gate, drain, and back-gate voltages.

The first issue that arises from calculating (3) is that the input voltage vector (amplitude and phase for all spectral components) is unknown. The Angelov compact model contains resistive, reactive, and nonlinear elements. This means that the solution of the circuit involves coupled, nonlinear, and frequency dependent equations. A commercial HB simulator is used to simulate the FET model and the control node voltages are exported and used as inputs for the DF method. By using HB, not only can the nonlinearity effects be calculated, but the total DF component results can be compared to the HB total component result for validation. Note however the important difference: HB gives total frequency content, while the DF approach includes information of specific interactions between signals.

As an example, a Gallium Nitride (GaN) FET has a measured low-frequency impedance at the drain as shown in Fig.2 [8]. An Angelov model extracted from the device shows a similar phenomenon in the drain impedance, but the mechanism for the peaking is difficult to understand and a more intuitive description would be useful to understand how to control this behavior.

Equation (3) is extended to a 3-dimensional nonlinearity and Python code was implemented to compute the result. Integration was performed with, `Cubature`, a multi-dimensional

integration library<sup>1</sup>. The FET was simulated in ADS with five harmonics plus mixing products (up to order 5). The gate, drain, and back-gate voltages were exported and used with the describing function code. To shorten the time for integration of the DF, the bias and a small selection of tones were used (chosen based on relevance to the total solution):  $\vec{f} = [10e6, 9.99e9, 10e9, 10.01e9]$  Hz. The complex drain impedance is calculated as  $Z_d = V_d/I_d$  using the following steps:

- HB is used to simulate the Angelov model with a 10 GHz fundamental on the gate and 10 MHz tone on the drain;
- the control voltages are exported which provide the inputs to (3);
- the describing function  $N_{\vec{k}}$  is numerically integrated;
- all order mixing products that land on the same frequency are summed;
- total DF response is compared to HB.

Fig. 3 shows the results of the DF output for the various mixing products for the drain current at 10 MHz compared to the total current as found by HB (dotted line). The numbers in the brackets correspond to the frequency mixing products as given by the vector of frequencies in the previous paragraph. For example, the primary (and majority of the current) component comes from the 10 MHz signal injected at the drain (legend key  $\vec{k} = [1, 0, 0, 0]$ ). The second order mixing products which involve 10 GHz and one of the IM3 side tones, have a smaller effect but are increasingly significant at higher RF input powers. The sum of the DFs gives the black line in the plot which tracks closely to the HB result. At lower RF input powers DF are almost identical to the HB result. Fig. 4 shows the computed drain impedance,  $Z_d$ , for the total DF result and various subsets of the total DF result. If one just uses the primary 10 MHz tone to calculate  $Z_d$  (red dashed line), the result is very flat and does not exhibit the peaking characteristic as shown in Fig. 4. Adding the RF tone in addition to the 10 MHz tone (black line) gives a self-biasing effect when the transistor starts to compress, but the impedance bump is less than the HB result (solid black line). Whereas, the full DF result (adding in the second order mixing products) tracks closely to the HB result. The results are not identical because of a small numerical offset of the DF compared to the HB result (in Fig. 3 the results are nearly identical at low RF input power, however, with the very small drain voltage, the impedance difference becomes  $\approx 6 \Omega$ ).

The resulting conclusion that can be drawn is that the RF IM3 products mixing back down to LF provide a non-trivial decrease in current at the onset of saturation, thereby, increasing the drain node impedance. This effect can be tested by modifying one of the RF adjacent tones *at the gate* and simulating the resulting effect on the LF impedance. Using the same export node voltages and modifying the amplitude and phase of the 9.99 GHz tone at the gate gives drain impedance

<sup>1</sup>C code for the library is at <http://ab-initio.mit.edu/wiki/index.php/Cubature>. A Python wrapper can be found at <https://github.com/saullocastr/cubature>.

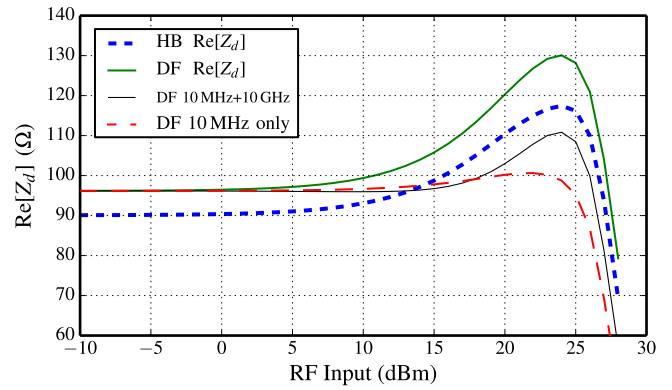


Fig. 4. (a) HB voltage used to calculate the (b) drain impedance. The comparison between HB and (total) DF  $Z_d$  is close both having very similar trends. If only the primary LF tone is used, the impedance does not have the large characteristic bump in impedance.

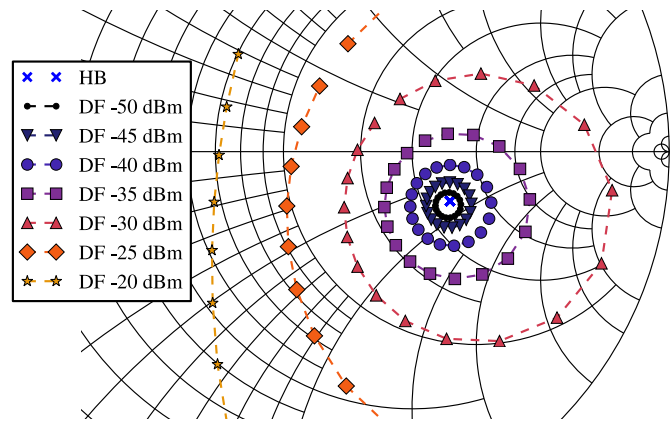


Fig. 5. LF impedance ( $Z_d$ ) of a FET when excited with 10 GHz and a 9.99 GHz tone is modified to have a set power (symbols) and phase (dotted line connecting symbols of certain type).

results shown in Fig. 5. With no modification, the device exhibits an impedance close to the blue ‘x’ shown in the plot (which is the HB solution as given from Fig. 4). As the 9.99 GHz tone power is increased, the impedance can be swept along a circular path roughly centered on the ‘x’ by means of the phase. The mixing product of the two RF tones (down to LF) is an output power with amplitude and phase that can be directly controlled.

A measurement bench was developed and a GaN FET was used to validate this phenomena using two RF tones at the gate while simultaneously measuring the low frequency mixing product [8]. The primary RF source at 10.7 GHz was set for an input power of 15 dBm. The low frequency impedance was measured at 20 MHz. Results of the measurement are shown in Fig. 6. The impedance with no power on the second RF tone is approximately 300  $\Omega$ . As the secondary tone power is increased and the phase swept, the same impedance modification effect is seen as in the simulated case. The LF impedance is centered around the 0 W input power case, and

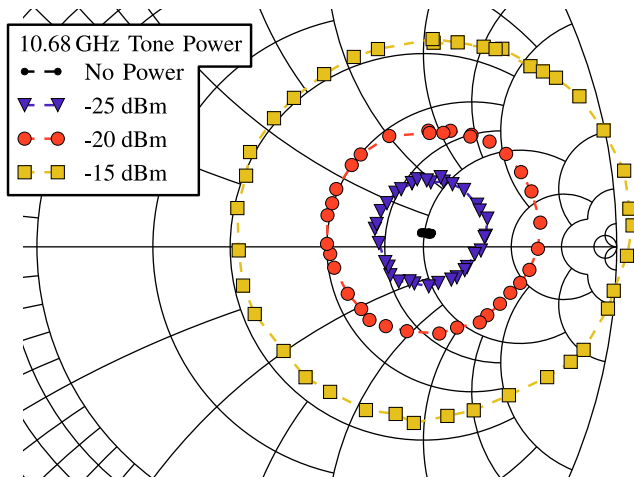


Fig. 6. Measured  $Z_d$  with a RF source of 10.7 GHz and a secondary RF source at 10.68 GHz with power given in the legend. The same LF impedance modification effect is seen as in DF and HB simulations.

larger radius circles are given by swept angle at a particular power of the RF tone. Note that the input powers for the secondary tone cannot be compared between the simulated and measured case: the simulated case sets the power at the internal gate control node assuming voltage across a  $50 \Omega$  load while the measured case is the available power at the input of the FET.

One may note that the computed impedances over swept phase as shown by DF are not centered at the zero power point. This is because the HB control voltages for 24 dBm were used, only modifying the 9.99 GHz tone, instead of re-simulating in HB for each gate input power: all the remaining elements of the Angelov model were ignored when directly modifying the 9.99 GHz tone. If the control voltages for HB were used for each input power and phase, the shape would be almost identical to the measured case.

This “active” impedance modification can be used directly with the measured LF impedance to predict the LF output waveform for wideband RF signals. Unfortunately, due to equipment limitations, the relative phase of the RF sources, which would be required to give the full picture of RF  $\rightarrow$  LF mixing, could not be measured.

#### IV. CONCLUSION

In summary, describing functions are shown to be a useful approach for accurate description of the multi-frequency mixing products of a GaN FET under supply modulation. DF allows analyzing outputs at higher mixing orders without and increase in complexity, either in code or extraction time. This paper presents the DF formulation, and shows results for the dependence of the low-frequency (10 MHz) drain impedance with a large-signal RF (10 GHz) input power. The inputs to the calculation are found from an available Angelov model and harmonic balance.

This paper detailed an example of exploring the mixing products down to low frequency of a supply modulated transistor under large signal RF drive. Understanding how RF tones mix down to low frequency allows better understanding of how the supply modulator can be used to negate the low frequency power for better linearity or inform DPD algorithms for wide-band supply modulation. The results show the same trends as observed in measurement.

#### V. ACKNOWLEDGMENT

This work was funded by ONR under the DARPA MPC Program N00014-11-1-0931. The authors are very grateful for the donation of equipment from National Instruments (Dr. Takao Inoue and Dr. Truchard).

#### REFERENCES

- [1] J. Bussgang *et al.*, “Analysis of Nonlinear Systems with Multiple Inputs,” *Proc. IEEE*, vol. 62, no. 8, pp. 1088–1119, Aug 1974.
- [2] M. Schetzen, *The Volterra and Wiener theories of nonlinear systems*. John Wiley & Sons, 1980.
- [3] P. Wambacq and W. Sansen, *Distortion Analysis of Analog Integrated Circuits*, ser. The Springer International Series in Engineering and Computer Science. Springer, May 1998.
- [4] S. Maas, *Nonlinear Microwave and RF Circuits*, ser. Artech House Microwave Library. Artech House, 2003.
- [5] A. Gelb and W. Vander Velde, *Multiple-input describing functions and nonlinear system design*, ser. McGraw-Hill electronic sciences series. McGraw-Hill, 1968.
- [6] N. Carvalho and J. Pedro, “Large- and Small-Signal IMD Behavior of Microwave Power Amplifiers,” *IEEE Trans. Microw. Theory Techn.*, vol. 47, no. 12, pp. 2364–2374, Dec. 1999.
- [7] I. Angelov *et al.*, “On the Large Signal Evaluation and Modeling of GaN FET,” *IEICE Transactions on Electronics*, vol. 93, no. 8, pp. 1225–1233, Aug 2010.
- [8] S. Schafer and Z. Popović, “Multi-Frequency Measurements for Supply Modulated Transmitters,” *IEEE Trans. Microw. Theory Techn.*, vol. 63, no. 9, pp. 2931–2941, Sep. 2015.